HHS Public Access

Author manuscript

Nano Lett. Author manuscript; available in PMC 2019 October 29.

Published in final edited form as:

Nano Lett. 2018 November 14; 18(11): 7021–7029. doi:10.1021/acs.nanolett.8b02989.

Nanothermometry Reveals Calcium-Induced Remodeling of Myosin

Eric R. Kuhn[†,⊥], **Akshata R. Naik**[†,⊥], **Brianne E. Lewis**[‡], **Keith M. Kokotovich**[†], **Meishan Li**[§], **Timothy L. Stemmler**[‡], **Lars Larsson**[§], **Bhanu P. Jena**[*,†]

[†] Department of Physiology, School of Medicine, Wayne State University, Detroit, Michigan 48201, United States

[‡] Department of Pharmaceutical Science, College of Pharmacy, Wayne State University, Detroit, Michigan 48201, United States

[§] Department of Physiology and Pharmacology, Karolinska Institutet, SE-171 77 Stockholm, Sweden

Abstract

Ions greatly influence protein structure–function and are critical to health and disease. A 10, 000-fold higher calcium in the sarcoplasmic reticulum (SR) of muscle suggests elevated calcium levels near active calcium channels at the SR membrane and the impact of localized high calcium on the structure–function of the motor protein myosin. In the current study, combined quantum dot (QD)-based nanothermometry and circular dichroism (CD) spectroscopy enabled detection of previously unknown enthalpy changes and associated structural remodeling of myosin, impacting its function following exposure to elevated calcium. Cadmium telluride QDs adhere to myosin, function as thermal sensors, and reveal that exposure of myosin to calcium is exothermic, resulting in lowering of enthalpy, a decrease in alpha helical content measured using CD spectroscopy, and the consequent increase in motor efficiency. Isolated muscle fibers subjected to elevated levels of calcium further demonstrate fiber lengthening and decreased motility of actin filaments on myosin-functionalized substrates. Our results, in addition to providing new insights into our

[*]**Corresponding Author** bjena@med.wayne.edu.

[⊥]Author Contributions

E.R.K. and A.R.N. contributed equally to this work. B.P.J. developed the idea, E.R.K., A.R.N., and B.P.J. designed experiments for the study. E.R.K., K.M.K., and A.R.N. conducted the experiments and analyzed the data. M.L. and L.L. conducted the experiments pertaining to myosin motility, analyzed, and presented the data. E.R.K., A.R.N., B.E.L., and T.L.S. conducted the experiments pertaining to CD spectroscopy and analyzed the data. E.R.K. and B.P.J, wrote the manuscript. All authors participated in discussions and proofread the manuscript.

The authors declare no competing financial interest.

ASSOCIATED CONTENT

Supporting Information

The Supporting Information is available free of charge on the ACS Publications website at DOI: 10.1021/acs.nanolett.8b02989. Cadmium telluride quantum dots adhered to myosin molecules function as nanoscale thermometers; circular dichroism spectroscopy of rabbit skeletal myosin confirms unwinding of the α helix; calcium mediated structural changes in myosin enable close interaction between the molecules as indicated by their ability to cross-link in the presence of paraformaldehyde; thin layer chromatography of ATP hydrolysis demonstrating no significant change in the ratios of ATP to hydrolyzed ADP in the presence of different calcium concentrations; secondary structure fit parameters of bovine cardiac myosin in the presence and absence of various increasing concentrations of calcium; secondary structure fit parameters of rabbit skeletal myosin in the presence and absence of various increasing concentrations of calcium; actin on myosin motility assay demonstrating no significant change in velocity at lower concentrations of calcium and a significant change at 5 mM calcium (PDF)

understanding of muscle structure–function, establish a novel approach to understand the enthalpy of protein–ion interactions and the accompanying structural changes that may occur within the protein molecule.

Graphical Abstract

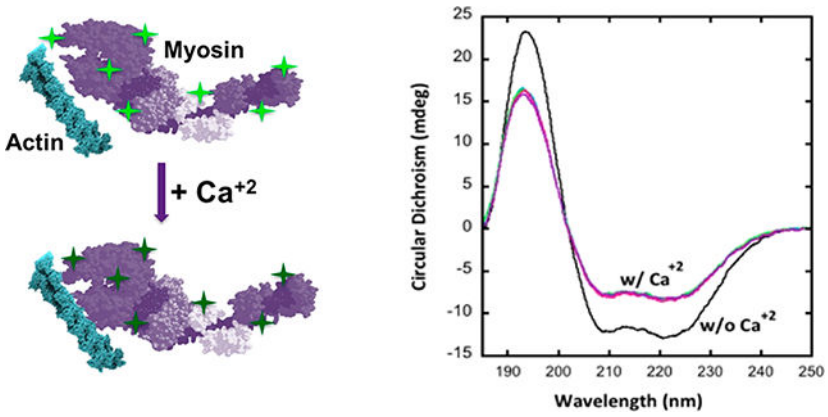

Keywords

Quantum dot thermometry; molecular motor myosin; calcium; muscle function

Muscle contraction is essential for proper physiological functioning from the beating of the heart to locomotion, involving calcium interaction with myosin.[1–4] Muscle contraction occurs by the sliding action of the thick and thin filaments, driven by ATP hydrolysis. While the regulation of contraction by the thin filament with the binding of calcium to troponin C and exposure of myosin binding sites has been well documented, less is known regarding the effects of calcium on the thick filament. In 1967, work by Huxley's group revealed distinct changes in the X-ray diffraction signatures of frog Sartorius muscle fibers after contraction,[5] identifying the characteristic helical pitch of myosin cross bridges in a 6/2 helix with a pitch of 42 nm. Furthermore, they demonstrated that there is a radial reorientation of the cross bridges during muscle contraction. In a recently published study[3] using X-ray diffraction, muscle activation and contraction were found to be controlled, in part, by the activation of the thick filament. Specifically, the ON and OFF structures of myosin, dictated by stretch, corresponded to increased and decreased interaction with the thin filament, respectively. While some myosin heads are ON constitutively, heads in the OFF state are sequestered in helical tracks. However, activation of the thick filament is characterized by increases in thick filament length and periodicity,[3,5] resulting in an increased association of myosin heads with the thin filament.[3] In light of studies demonstrating the release of calcium with stretching of smooth muscle as well as the role of stretch activated channels in calcium accumulation in skeletal muscle,[6] we hypothesize that the trigger for this mechanosensing capability in muscle activation is calcium.

In several myosin isoforms, self-regulation is thought to be mediated by the lever arm, where the regulatory light chain (RLC) and essential light chain (ELC) are located.[7] Both light chains are members of the EF hand calcium binding family. This family contains a number

of helix-turn-helix calcium binding domains, similar to troponin C and calmodulin, suggesting its participation in calcium binding.[8,9] Scatchard plot analysis has demonstrated at least 1–2 high affinity binding sites with numerous other lower affinity sites that likely mediate the calcium response.[10] Although calcium is the preferred myosin ligand, magnesium too is reported to competitively bind to the motor protein, possibly to the same sites binding calcium. Magnesium modulates actin binding and ADP release in myosin. To understand the effect of elevated calcium on changes in myosin enthalpy and to the structure and function of the molecule, and determine whether magnesium and calcium binding sites on myosin are the same or different, the current study was undertaken.

Results and Discussion

In the current study, previously unknown energetics, conformational changes at the molecular level, and functional outcomes of the binding of calcium to myosin were investigated using nanothermometry, circular dichroism spectroscopy, and nanoscale motility assays. Utilizing a previously developed thermometry approach[11] that employes cadmium telluride quantum dots (CdTe-QDs) adhered to the substrate, we were able to detect changes in the temperature of the substrate as reflected in changes in fluorescence intensity. This approach allowed us to measure changes that the myosin experiences in the presence of increasing calcium and magnesium concentrations (Figure 1; see Supporting Information). Changes in temperature are inversely proportional to changes in fluorescence of the QDs. Fluorimetric measurements in real-time of myosin-associated CdTe-QDs in solution exhibit increased heat loss in the presence of increasing calcium concentrations, demonstrating that calcium lowers the enthalpy of myosin (Figure 1). Bovine cardiac (BC) myosin (Figure 1) and rabbit skeletal (RS) myosin (Figure 1S) both show an immediate and steep decrease in QD fluorescence in the presence of calcium, implying an exothermic process and a decrease in the enthalpy of the molecular motor and thus the transition of the molecule to a more stable lower energy state. The heat loss by myosin is calcium dose-dependent, showing a 32% drop in fluorescence, at a rate of approximately 1%/s in the first 30 s in the presence of 5 mM calcium, and up to a 52% drop (at a rate of approximately 1.7%/s) in the presence of 20 mM calcium (Figure 1a,c). In contrast, the total percent drop and rate of fluorescence loss in the presence of 5 mM, 10 mM, and 20 mM magnesium was attenuated (Figure 1b,d). To determine if the binding sites for calcium and magnesium on myosin are same or different, changes in the enthalpy of myosin first exposed to 10 mM calcium followed by 10 mM magnesium were examined. If the binding sites are the same for both the cations, there would be no further loss of fluorescence following addition of 10 mM magnesium to myosin-QDs pre-exposed to 10 mM calcium. However, if exposure to 10 mM magnesium resulted to a further loss of fluorescence following the initial exposure of myosin to 10 mM calcium, it would demonstrate the binding sites of calcium and magnesium in myosin to be different. As hypothesized, results from the study (Figure 2) support that both calcium and magnesium bind to the same sites on the myosin molecule. These results further suggest that the greater lowering of enthalpy of myosin on exposure to a certain concentration of calcium versus magnesium is due in-part to the high affinity of calcium for myosin over magnesium. Not surprising, therefore, earlier studies report a near three orders of magnitude in magnesium concentrations required to replace calcium from

myosin. Hence, calcium being the preferred cation for myosin binding sites, the binding of magnesium to the same sites is less than optimal, explaining the attenuated response of BC myosin to magnesium compared to calcium. Furthermore, results from thermometry experiments (Figure 1 and Supporting Information, Figure 1S) demonstrate that RS and BC myosin respond to different degrees in changes to their enthalpy following exposure to calcium and magnesium. Concentrations of 0, 5, 10, 15, and 20 mM calcium were chosen due to the likely high calcium concentrations near channel openings at the sarcoplasmic reticulum/T-tubule triad.[4,12] Therefore, it is likely that thick filaments adjacent to the sarcoplasmic reticulum's calcium channels are exposed to high local concentrations of calcium during muscle activity.

Proteins exist as ensembles of various conformations with different associated energy states. To explore possible structural changes associated with the observed loss in energy of the myosin molecule upon calcium binding, we analyzed the response of isolated mouse skeletal muscle fibers (Figure 3a–c) to 0, 1, and 10 mM calcium using immunohistochemistry and BC and RS myosin (Figure 3d; Supporting Information Figure 2S, Table 1S, Table 2S) in various calcium concentrations using circular dichroism (CD) spectroscopy. Myosin has a primarily helical structure as an apoenzyme with approximately 80% alpha helical content in the BC myosin and 56% alpha helical content in the RS myosin (Figure 3d; Supporting Information Figure 2S, Table 1S, Table 2S). Addition of calcium promoted a significant dose-dependent decrease in the helical content of myosin. While RS myosin demonstrated a 15% decrease in helical content and slight increases in β sheet and unfolded regions in the presence of 20 mM calcium, BC myosin demonstrated far greater sensitivity to addition when exposed to the cation, with a significant drop even at 5 mM Ca and a greater 27% drop in the presence of 20 mM calcium. The CD spectra allowed us to corroborate these structural changes with our observed transitions in enthalpy. These changes are likely occurring in the neck region of the myosin molecule since this is the location for binding of the regulatory and light chains, which mediate calcium binding. Additionally, the earlier small-angle X-ray diffraction studies carried out by Huxley showed activation involves the rotation of the heads away from the thick filament to interact with the actin binding sites. In further support of the extension of the neck region upon calcium binding, studies[13] reveal that in activating calcium concentrations, there is an increase in susceptibility of the myosin head-neck junction to papain digestion. Our CD results are in agreement with previously observed[5] structural changes in the overall length and periodicity of the myofilament. Previously reported small-angle X-ray diffraction studies[3] have demonstrated differences between the ON and OFF states of the thick filament where contraction has been associated with an increase in the axial distances of the myosin heads. Analogous to the unwinding of a spring, which results in an increase in diameter of the coil with a corresponding increase in length, greater interaction between myosin heads and actin could result in the presence of high calcium. Similar observations have been made in scallop myosin subjected to high calcium concentrations, resulting in the transition of the thick filament from a helical configuration to a more disordered state[13]. It may be that the calcium release during contraction is responsible for the activation and transition of the myosin heads from the OFF to the ON state. To further understand the effects on muscle fiber on the observed structural changes in myosin using CD, immunohistochemistry using myosin IIB specific antibody was

performed on isolated mouse skeletal muscle fibers exposed to high calcium. In the presence of elevated calcium levels (0 to 10 mM), a linear increase in muscle fibers is observed, as reflected in the significant increases in distances between the A bands (Figure 3a,b). Since 10 mM calcium was an intermediate concentration (between 5 mM and 20 mM) that demonstrates changes in the enthalpy and structure of myosin, it was chosen both for the calcium and magnesium binding site assays shown in Figure 2 and for the A band length assay in Figure 3. We further used paraformaldehyde cross-linking of the myosin in absence and presence of high calcium followed by SDS-PAGE and subsequent silver and Coomassie Brilliant Blue staining to determine the extent of intermolecular interactions. The presence of higher molecular weight bands in myosin exposed to calcium demonstrates closer interactions among individual myosin molecules, resulting in cross-linking by paraformaldehyde (Supporting Information, Figure 3S). It is likely that the increase in the disordered state of myosin in the presence of high calcium observed using CD allows for increased frequency of interactions compared to the tightly wound, calcium-free, helical state.

We were interested to understand the effect of this dramatic structural change in myosin on its function, both with respect to its hydrolytic activity and efficiency as well as its interaction with actin (Figure 4). To this end, efficiency studies were performed that evinced a clear dose-dependent increase in the efficiency of the BC myosin with increasing calcium levels (Figure 4a,b). Minimal heat loss occurred at a concentration of 20 mM calcium, whereas maximal heat loss occurred in the absence of any calcium. This increase in enzymatic efficiency of myosin may likely be due to conformational changes resulting in increased flexibility in the neck region of the motor. Thus, similar conformational changes that allow for the activation of myosin and its interaction with actin may allow for its improved efficiency. Because of reports of calcium decreasing ATPase activity in some myosin isoforms,[14] thin layer chromatography (TLC) controls were performed to ensure that the total amount of ATP hydrolyzed in the presence of different calcium concentrations was unchanged (Supporting Information Figure 4S). No significant difference was observed in the ratio of ADP to ATP at any given concentration of calcium, suggesting that decrease in heat loss from myosin hydrolysis of ATP at increasing calcium concentrations was solely due to an increase in myosin efficiency (Figure 4a,b).

Experiments where the neck region of the myosin molecule had been extended demonstrate a direct correlation between length of the lever arm and the velocity[15] in motility assays. However, there are other factors such as the dwell time of myosin with actin that can increase with increasing affinity between the molecules and thus influence the velocity. The dwell time, where myosin is associated with actin, is inversely correlated with the velocity according to the equation: $v = d/t_s$, where v is the velocity of the fibers in a motility assay, d is the length of the lever arm (step distance), and t_s is the dwell time.[16] Molecular dynamic simulations show that with an increase in calcium concentration there is greater association of myosin with actin,[17] demonstrating increasing affinity of myosin for actin at higher calcium concentrations. This would suggest that calcium could influence both the structure of the myosin molecule (Figure 3d; Supporting Information, Figure 2S, Table 1S, Table 2S) as well as its binding affinity to actin, resulting in either an increase in step size or an increase in dwell time. Depending on these parameters (step size and dwell time), there

would be an increase or decrease in motility. Since we have seen in our experiments, using both CD as well as isolated fibers, an increase in linear length of an isolated muscle fiber (Figure 3a–c) and uncoiling of the α helix in myosin molecules in the presence of elevated calcium (Figure 3d; Supporting Information Figure 2S, Table 1S, Table 2S), this suggests either possibility. In cases where the neck region is longer, the motility will be faster. However, if the myosin-actin dwell time is extended, it will result in a decrease in velocity. To be able to determine the effect of increasing calcium concentrations on velocity, we performed motility assays[18] (Figure 4c,d; Supporting Information, Table 3S). Interestingly, we found relatively little change at lower calcium concentrations on actin velocity; however, at higher calcium concentrations (5 mM), a loss of velocity was observed, suggesting that the predominant factor in the lowering of motility is likely increased dwell time.

Earlier studies report a thermodynamic trade-off between precision and speed in molecular motors.[19,20] Myosin ATPase activity and cross bridge cycling are dissipative processes and stochastic in nature; thus, there is a certain degree of error associated with them, governed by the thermodynamic uncertainty relation.[21] In myopathy, for example, there is a switch from slow (more efficient) to fast twitch muscle.[22,23] The thermodynamic uncertainty relation, Q, is constant for a motor and is the product of the energy dissipation and the error associated with the process. A more efficient motor is optimized where there is a speed trade-off to minimize energy expenditure and reduce error, hence increased precision.

Our motility assays show an approximate 33% loss in motility at 5 mM calcium (Figure 4d; Supporting Information, Table 3S); however, the same calcium concentration shows a nearly 60% increase in myosin efficiency (Figure 4a,b). Considering that the loss in motility is relatively small and the decrease in energy loss is comparatively greater, the molecular motor is optimized at higher calcium concentrations (Figure 5). Additionally, the motility may be influenced by the regulatory role of myosin binding protein C, present in the intact muscle tissue. While MyBP-C can have an activating effect on the rate of force development and velocity, this can be switched to an inactivating effect in the presence of high concentrations of calcium.[24–26]

Conclusion

In summary, results from the current study establish a new paradigm in muscle structure–function in that in addition to the classical role of calcium in thin filament regulation, direct binding of the ion at elevated levels to myosin results in lowering the enthalpy of the molecule (Figure 5S), resulting in a decrease in alpha helical content within the motor protein, promoting its interaction with actin and in improved efficiency. Additionally, our study suggests that both calcium and magnesium likely bind to the same site on the myosin molecule, calcium binding at a much higher affinity than magnesium. It is possible that additional high affinity binding sites for magnesium exist in myosin since magnesium modulates actin binding and ADP release in myosin. Our study also demonstrates a trade-off between speed and precision in the motor function, with precision and efficiency at higher calcium and a concomitant loss of the sliding velocity of actin filaments on myosin. Results from the current study reveal an entirely novel role of calcium on muscles, contributing to a new paradigm in our understanding of muscle structure–function. Future studies on the

binding affinities of the calcium binding domains of myosin and their role in myosin structure–function will provide a greater understanding of the effects of elevated calcium on muscle contraction. As magnesium has been reported to be important in muscle contraction[27–30] and calcium and magnesium have been suggested to bind to the same sites, greater insight into how the binding of both ions impact muscle function will be revelatory. Additionally, this novel approach of QD-based nanoscale thermometry provides a powerful tool to detect and study changes in the enthalpy of ion-binding protein molecules when exposed to specific ions to which they have binding sites (Figure 5S), resulting in changes to their structure–function. In addition to protein–ion interactions, QD-mediated enthalpy changes could be used to study a wide range of biomolecular interactions such as protein–protein, protein–lipid, and protein–nucleic interactions, providing a wealth of information on their structure–function. Signatures of QD-based thermal shifts of ion-binding proteins can be explored for proteins identification, and similarly, the interactions between proteins within a supramolecular complex could be determined, providing critical information on the molecular architecture of such complexes. Furthermore, using QD-based nanoscale thermometry, one could study in real-time the energetics of folding and unfolding of proteins and differentiate normal from transformed cells[11] (increased glycolytic over oxidative metabolism in cancer cells result in greater heat loss) and various bacterial pathogens, reflecting on the wide spectrum of applications of this direct-adhesion QD-based approach of nanoscale thermometry.

Materials and Methods

Nanothermometry

The use of 2 nm CdTe QDs obtained from Sigma-Aldrich as nanoscale thermometers was characterized and used according to our published[11] procedure. Ten milligrams of −COOH functionalized CdTe core-type QDs with reported average size of 2.04 nm and λ_{em} = 520 nm (Lot # MKBZ9296 V, Sigma-Aldrich) was diluted in 2 mL of deionized double distilled and filtered water to obtain a 5 mg/mL stock solution and stored in the dark at 4 °C. Using a Zetasizer Nano ZS (Malvern Instruments, U.K.), photon correlation spectroscopy (PCS) was performed to determine the size distribution of the QDs at various dilutions of the suspension. PCS measurements were performed on the size distribution of QDs by the Zeta sizer using built-in software provided by Malvern Instruments. Prior to the determination of the hydrodynamic radius of the QDs, the instrument was calibration using latex spheres of known size. In PCS, subtle fluctuations in the sample scattering intensity were correlated across microsecond time scales, and the correlation function was calculated from which the diffusion coefficient was determined. Using Stokes–Einstein equation, hydrodynamic radius can be acquired from the diffusion coefficient. The intensity size distribution, which was obtained as a plot of the relative intensity of light scattered by particles in various size classes, was then calculated from a correlation function using built-in software and found to be 2.04 nm (single sharp peak) for the CdTe QDs. As previously published,[11] once the QD size was established and matched the specifications provided by the company (Sigma-Aldrich), the size of myosin in suspension was estimated using the Zetasizer and determined to be 24 nm (single peak with a 20–32 nm distribution). According to our published[11] procedure, to achieve optimal binding of QDs to myosin molecules and to establish 100%

binding (no unbound QDs that would provide background fluorescence), incremental amounts of QDs were added to a fixed amount of myosin (100 μg) and the size of suspended particles accessed using the Zetasizer when at the highest concentration of QDs (15 μg) just one peak was observed (28 nm).[11] Briefly therefore to prepare myosin-QDs, 1 mg of myosin (MYO)protein (Cytoskeleton, Inc., Denver, CO) was diluted in 100 μL of myosin resuspension buffer (15 mM Tris-HCl pH 7.5) to obtain a final concentration of 10 mg/mL. Ten microliters of myosin protein (10 mg/mL) was incubated with 3 μL of CdTe QDs (5 mg/mL) for 30 min to obtain MYO-QDs and the 100% binding of QDs to MYO as previously[11] determined using the Zetasizer. The temperature changes of bovine cardiac and rabbit skeletal myosin in varying ionic solutions were evaluated using a F-2000 Hitachi fluorescence spectrophotometer in a 0.5 cm quartz cuvette. Myosin was reconstituted to a concentration of 10 mg/mL, and 3 μL of a −COOH functionalized CdTe core-type QD solution (Sigma-Aldrich) was added to the reconstituted myosin. This was allowed to sit in darkness for 30 min prior to fluorimetry analysis. Quantum dots were excited with 350 nm (λ_{ex} = 350 nm), and fluorimetry emission readings were taken at 520 nm over a period of 150 s. Addition of ionic solutions occurred at 60 s, and measurements for each calcium/magnesium concentration were done in triplicate. Each sample had a final concentration of 15 μg/mL in 100 mM TRIS buffer at pH 7.4. TRIS solution was made with deionized H_2O to minimize ionic salts in the samples.

Circular Dichroism Spectroscopy

Overall, secondary structural content of myosin isoforms in varying ionic solutions was determined using a Jasco 1500 spectrometer and a 0.01 mm quartz cuvette (Hellma). An average of 30 scans were collected in total for each sample from triplicate preparations for an enhanced signal-to-noise ratio. The following samples were analyzed: bovine cardiac (BC) myosin + 0 mM $CaCl_2$, BC myosin + 5 mM $CaCl_2$, BC myosin + 10 mM $CaCl_2$, BC myosin + 15 mM $CaCl_2$, BC myosin + 20 mM $CaCl_2$. Additionally, rabbit skeletal myosin (RS) + 0 mM $CaCl_2$, RS myosin + 5 mM $CaCl_2$, RS myosin + 10 mM $CaCl_2$, and RS myosin + 15 mM $CaCl_2$ were analyzed. Each sample had a final concentration of 10 μM myosin in 5 mM TRIS buffer at pH 7.4 and was baseline-subtracted to eliminate buffer signal. Data were analyzed using CDPro analysis software and fit with the CONTIN method and SP29, SP37, SP43, SMP50, and SMP56 reference sets.

Immunohistochemistry

Mouse skeletal muscle tissue was used to perform whole mount immunohistochemistry. Tissues were teased out on 35 mm glass bottom Petri dishes and incubated for 5 min with three different concentrations of $CaCl_2$: 0 mM, 1 mM, and 10 mM. Myosin IIB fibers were stained with a 1:200 dilution of a mouse monoclonal heavy chain primary antibody in each plate and subsequently incubated with a 1:500 dilution of AF 488 donkey antimouse as the secondary antibody. An immunofluorescence FSX100 Olympus microscope was used to acquire immuno-fluorescent images through a 63× objective lens (numerical aperture, 1.40) with illumination at 488 nm. The protein Myosin IIB distribution was attained through the processing on the images on the software, ImageJ. To minimize measurement error, the linear lengths for 10 to 20 bands were collected and divided by the number of bands to

obtain band distances, which resulted in calculated p-value of <0.005 of band distances between control and experimental values.

Nanothermometry Measurement of Efficiency

Efficiency of bovine cardiac myosin was determined using a F-2000 Hitachi fluorescence spectrophotometer in a 0.5 cm quartz cuvette. Myosin was reconstituted in double distilled water and incubated with a 5 mg/mL quantum dot solution for 30 min prior to fluorimetric analysis. Then 1.25 μL aliquots of this solution were added to varying volumes of 100 mM TRIS and brought up to a correct concentration of calcium. It was further allowed to equilibrate for 60 s with a stirrer. The sample was then excited at 350 nm light and the emission recorded at 520 nm over a period of 150 s. At 30 s into the time scan, 21 μL of 100 mM ATP in 100 mM TRIS was aliquoted into the cuvette and the online real-time fluorescence intensity recorded.

Thin Layer Chromatography

To control for any possible effect by the calcium concentrations on ATPase activity of myosin, thin layer chromatography was performed. Solutions of myosin in TRIS buffer were prepared to specific calcium concentrations of 0, 5, 10, 15, and 20 mM. ATP was then aliquoted into each reaction mixture and allowed to react for 15 s prior to quenching with blebbistatin (Sigma-Aldrich, St. Louis, MO, USA), a myosin ATPase inhibitor. Fifteen microliter aliquots were taken from each solution and blotted onto a cellulose thin layer chromatography plate. This was run in a glass chamber saturated with a mobile phase of 1 M lithium chloride in H_2O. Spot intensity was photographed under UV illumination to identify ATP and ADP. The ratio of ADP to ATP was analyzed with ImageJ software.

Extraction of Myosin and Motility Assay[18]

A short muscle fiber segment (1e2 mm) was placed on a glass slide between two strips of grease and a glass coverslip placed on top, creating a flow cell of ~2 mL. Myosin was extracted from the fiber segment through addition of a high-salt buffer (0.5 M KCI, 25 mM Hepes, 4 mM $MgCl_2$, 4 mM EGTA, and the pH value was adjusted to 7.6 before adding 2 mM ATP and 1% β-mercaptoethanol). After 30 min incubation on ice, a low-salt buffer (25 mM KCl, 25 mM Hepes, 4 mM $MgCl_2$, 1 mM EGTA, and the pH value was adjusted to 7.6 before adding 1% b-mercaptoethanol) was applied. The pH of the buffers was adjusted with KOH, and the final ionic strength of the motility buffer was 71 mM. After rhodamine-phalloidin (RH-PH, Invitrogen, Carlsbad, CA, USA) labeled actin was incubated with extracted myosin in varying calcium concentrations, the fluorescence strip was imaged from the muscle fiber and the in the flow cell. When the motility was successfully established, the direction of moving filaments relative to the x-axis, in both central and outer regions, was analyzed in the same preparation.

Supplementary Material

Refer to Web version on PubMed Central for supplementary material.

Funding

Funding work presented in this article was supported in part by the National Science Foundation Grant No. CBET1066661 (B.P.J.), the WSU Interdisciplinary Biomedical Systems Fellowship (A.R.N.), and the Erling-Persson Family Foundation, the Swedish Research Council Grant No. 8651, and the Stockholm City Council Grant Nos. Alf 20150423 and 20170133 (L.L.).

REFERENCES

(1). Reconditi M Motion of myosin head domains during activation and force development in skeletal muscle. Proc. Natl. Acad. Sci. U. S. A 2011, 108, 7236–7240. [PubMed: 21482782]

(2). Gordon AM; Homsher E; Regnier M Regulation of contraction in striated muscle. Physiol. Rev 2000, 80, 853–924. [PubMed: 10747208]

(3). Linari M; et al. Force generation by skeletal muscle is controlled by mechanosensing in myosin filaments. Nature 2015, 528, 276–279. [PubMed: 26560032]

(4). Toyoshima C How Ca^{2+}-ATPase pumps ions across the sarcoplasmic reticulum membrane. Biochim. Biophys. Acta, Mol. Cell Res 2009, 1793 (6), 941.

(5). Huxley HE; Brown W The low-angle x-ray diagram of vertebrate striated muscle and its behaviour during contraction and rigor. J. Mol. Biol 1967, 30, 383–434. [PubMed: 5586931]

(6). Sonobe T; Inagaki T; Poole DC; Kano Y Intracellular calcium accumulation following eccentric contractions in rat skeletal muscle in vivo: role of stretch-activated channels. Am. J. Physiol Regul Integr Comp Physiol 2008, 294, R1329–R1337. [PubMed: 18199588]

(7). Umeki N The tail binds to the head-neck domain to form a folded-back conformation that inhibits the actin-activated ATPase activity of Drosophila myosin VIIA. Biophys. J 2009, 96 (3), 1. [PubMed: 18849411]

(8). Da Silva ACR; et al. Determinants of ion specificity on EF-hands sites. J. Biol. Chem 1995, 270, 6773–6778. [PubMed: 7896823]

(9). Fromherz S; Szent-Gyorgyi AG Role of essential light chain EF hand domains in calcium binding and regulation of scallop myosin. Proc. Natl. Acad. Sci. U. S. A 1995, 92, 7652–7656. [PubMed: 7644472]

(10). Bremel RD; Weber A Calcium binding to rabbit skeletal myosin under physiological conditions. Biochim. Biophys. Acta, Bioenerg 1975, 376, 366–374.

(11). Laha S; et al. Nanothermometry measure of muscle efficiency. Nano Lett. 2017, 17, 1262–1268. [PubMed: 28112520]

(12). Langer G. a.; Peskoff A Calcium Concentration and Movement in the Diadic Cleft Space of the Cardiac Ventricular Cell. Biophys. J 1996, 70, 1169–1182. [PubMed: 8785276]

(13). Frado LL Structural changes induced in Ca^{+2}-regulated myosin filaments by Ca^{+2} and ATP. J. Cell Biol 1989, 109, 529–538. [PubMed: 2760106]

(14). Zhang Y; et al. Calcium regulation of the ATPase activity of Physarumand scallop myosins using hybrid smooth muscle myosin: The role of the essential light chain. FEBS Lett. 2010, 584, 3486–3491. [PubMed: 20633559]

(15). Uyeda TQ; Abramson JD; Spudich JA The neck region of the myosin motor domain acts as a lever arm to generate movement. Proc. Natl. Acad. Sci. U. S. A 1996, 93, 4459–4464. [PubMed: 8633089]

(16). Spudich JA How molecular motors work. Nature 1994, 372, 515–518. [PubMed: 7990922]

(17). Geeves M; et al. Cooperative [Ca^{+2}]-dependent regulation of the rate of myosin binding to actin: Solution data and the tropomyosin chain model. Biophys. J 2011, 100, 2679–2687. [PubMed: 21641313]

(18). Li M; et al. Nanometric features of myosin filaments extracted from a single muscle fiber to uncover the mechanisms underlying organized motility. Arch. Biochem. Biophys 2015, 583, 1–8. [PubMed: 26116379]

(19). Hwang W; Hyeon C Energetic costs, precision, and efficiency of a biological motor. J. Phys. Chem. Lett 2018, 9, 513–520. [PubMed: 29329502]

(20). Efremov A; Wang Z Universal Optimal Working Cycles of Molecular Motors. Phys. Chem. Chem. Phys 2011, 13 (13), 6223. [PubMed: 21359395]

(21). Barato AC; Seifert U Thermodynamic uncertainty relation for biomolecular processes. Phys. Rev. Lett 2015, 114, 158101. [PubMed: 25933341]

(22). Takikita S; et al. Fiber type conversion by PGC-1α activates lysosomal and autophagosomal biogenesis in both unaffected and Pompe skeletal muscle. PLoS One 2010, 5, e15239. [PubMed: 21179212]

(23). Reed UC; et al. Rod distribution and muscle fiber type modification in the progression of Nemaline myopathy. Journal of Child Neurology 2003, 18, 235–240. [PubMed: 12731651]

(24). Irving M Regulation of contraction by the thick filaments in skeletal muscle. Biophys. J 2017, 113, 2579–2594. [PubMed: 29262355]

(25). Hofmann PA; Greaser ML; Moss RL C-protein limits shortening velocity of rabbit skeletal muscle fibres at low levels of Ca^{2+} activation. J. Physiol 1991, 439, 701–715. [PubMed: 1895247]

(26). Korte FS; et al. Loaded shortening, power output, and rate of force redevelopment are increased with knockout of cardiac myosin binding protein-C. Circ. Res 2003, 93, 752–758. [PubMed: 14500336]

(27). Mccully KK; et al. The Reproducibility of Measurements of Intramuscular Magnesium Concentrations and Muscle Oxidative Capacity Using 31P MRS. Dyn. Med 2009, 8 (1), 5. [PubMed: 20003509]

(28). Skov M; et al. Extracellular Magnesium and Calcium Reduce Myotonia in ClC-1 Inhibited Rat Muscle. Neuromuscular Disorders 2013, 23 (6), 489–502. [PubMed: 23623567]

(29). Swenson AM Magnesium Modulates Actin Binding and ADP Release in Myosin Motors. J. Biol. Chem 2014, 289 (34), 23977–23991. [PubMed: 25006251]

(30). Fujita-Becker, Setsuko Changes in Mg2 Ion Concentration and Heavy Chain Phosphorylation Regulate the Motor Activity of a Class I Myosin. J. Biol. Chem 2004, 280 (7), 6064–6071. [PubMed: 15579903]

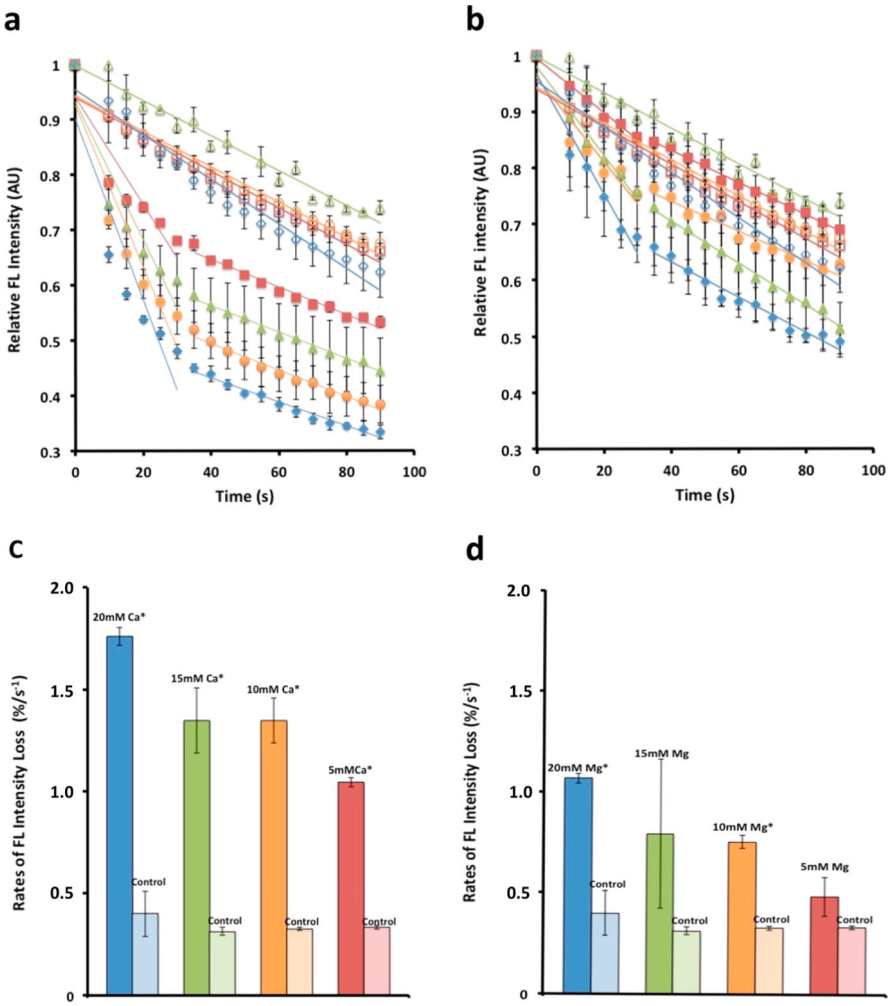

Figure 1.

Cadmium telluride quantum dots adhered to myosin molecules function as nanoscale thermometers, enabling the detection of heat loss from the motor protein on binding to calcium or magnesium. Binding of calcium to bovine cardiac (BC) myosin lowers the enthalpy of the molecule to a greater degree than magnesium. (a–d) Binding of calcium to bovine cardiac (BC) myosin lowers the energy state of the motor protein greater than magnesium. (a) Cadmium telluride quantum dots associated with the myosin molecule and used as molecular thermometers are able to detect mK changes in temperature of the myosin molecule. Changes in temperature are reflected as a change in fluorescence. The greater the heat loss, the lower the fluorescence.[11] Calcium concentrations used were 5 mM (solid red squares), 10 mM (solid green triangles), 15 mM (solid orange circles), and 20 mM (solid blue diamonds). Color coded corresponding controls were empty symbols. This calcium and magnesium dependent drop in fluorescence is a measure of heat release. Real-time fluorimetry demonstrates the extent and rate of this heat loss. (b) There is similarly a magnesium dependent drop in fluorescence, however, to a lesser extent than calcium. (c, d) Rate of fluorescence loss in the first 30 s following addition of calcium or magnesium. (c) Note that the rate of heat release in the presence of increasing calcium concentration is 30% greater than is observed with (d) magnesium. (Data presented is MEAN ± SEM, $n = 3$, $*p <$

0.005). Similar study using rabbit skeletal (RS) myosin is presented in Figure 1S (Supporting Information).

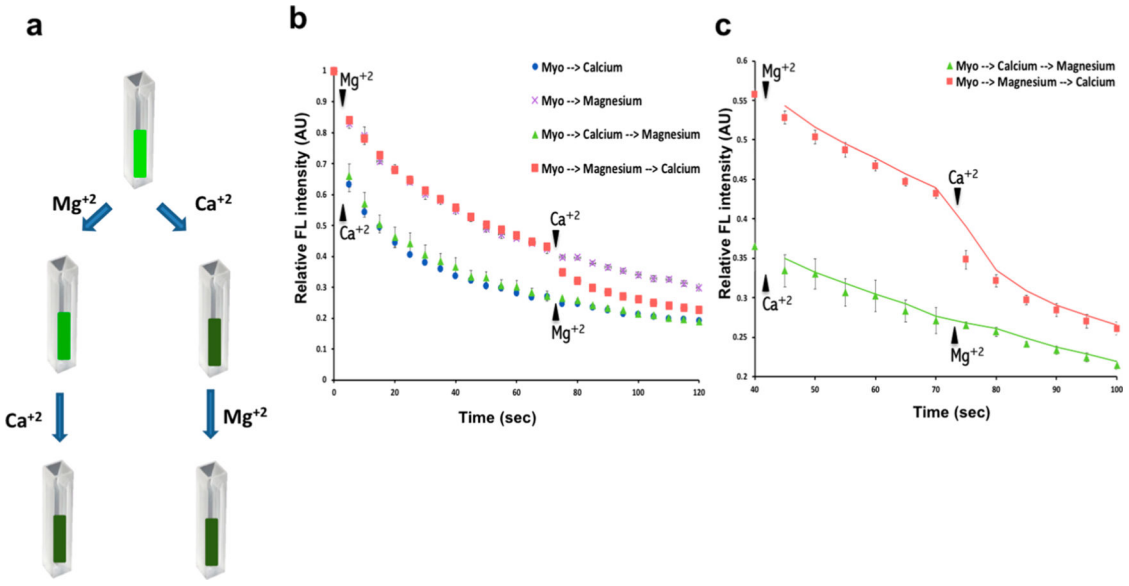

Figure 2.

Calcium and magnesium share the same binding sites in the myosin molecule. (a) Schematic drawing of the experiment showing that myosin pre-exposed to 10 mM calcium demonstrate little change in the enthalpy following exposure to 10 mM magnesium. In contrast, myosin preexposed to 10 mM magnesium demonstrate a near 10% drop in the enthalpy following exposure to 10 mM calcium. (b) Spectrofluorimetric measurements of time-dependent loss in fluorescence when myosin pre-exposed to 10 mM magnesium is followed by exposure to 10 mM calcium. Little change in enthalpy is observed when myosin pre-exposed to 10 mM calcium is followed by exposure to 10 mM magnesium, demonstrating that the loss of enthalpy of myosin is not additive when the motor protein is first exposed to calcium followed by magnesium addition (data presented is MEAN ± SEM, $n = 3$). (c) Section of Figure 2b has been rescaled for clarity. These results suggest that calcium and magnesium likely share the same binding sites on myosin and that calcium has a greater binding affinity to myosin than magnesium.

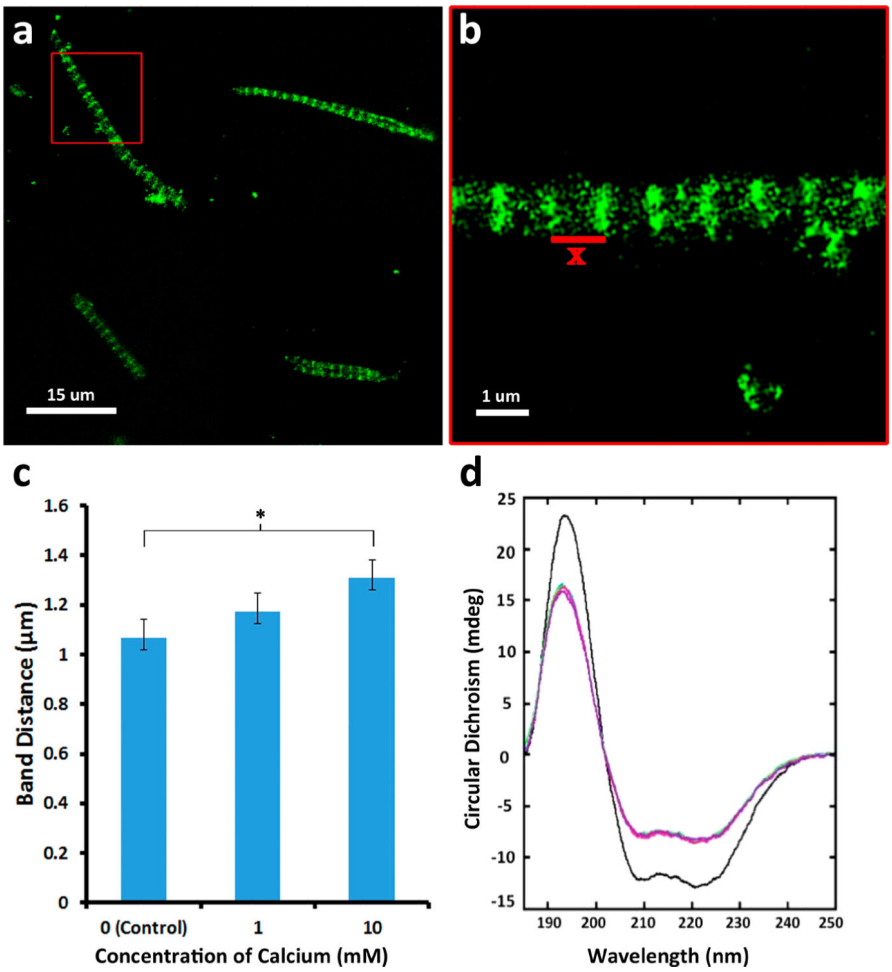

Figure 3.

Myosin undergoes structural changes in the presence of elevated calcium. (a, b) Mouse muscle fibers exposed to calcium results in approximately a 10% increase in the distance between the A bands (data presented are MEAN ± SEM, $n = 5$). (c) Dose-dependent increase in A band distances (*$p < 0.005$). (d) Circular dichroism spectroscopy of BC myosin demonstrates unwinding of the α helix (Supporting Information, Table 1S). Calcium concentrations used are 0 mM (black), 5 mM (blue), 10 mM (green), and 15 mM (red). An average of 30 scans were collected in total for each sample from triplicate preparations.

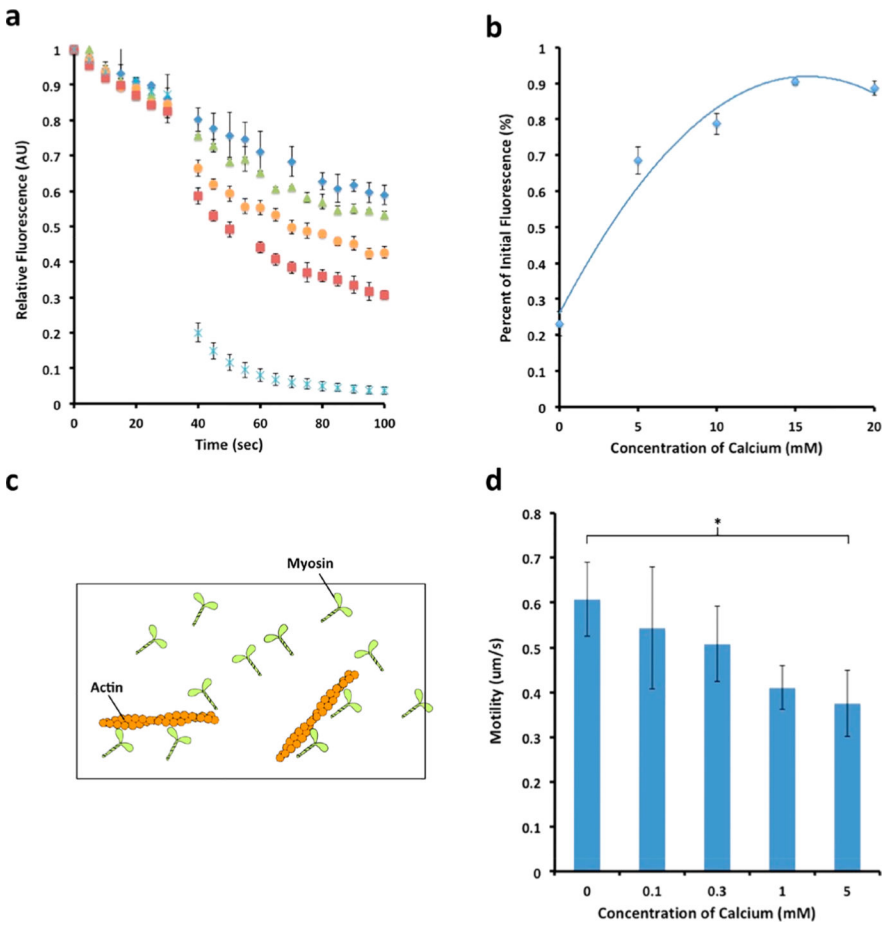

Figure 4.

Calcium-dependent increase in myosin efficiency and its impact on motility. (a) Molecular motor myosin consumes energy in the form of ATP for mechanical work. The greater the heat loss in the hydrolysis of ATP by myosin, less is available for mechanical work and hence lower the efficiency (data presented are MEAN ± SEM, $n = 4$). Note the lower heat loss at higher calcium concentrations, hence greater efficiency. (b) Plot of panel a showing calcium dose dependence retention of fluorescence, hence less heat loss at increased calcium concentrations. (c) Schematic diagram of a motility assay setup. Myosin attached to the surface of the coverslip is used to observe and measure motility of fluorescently labeled actin filaments. (d) Myosin motility assay demonstrates decreased motility with increased calcium (see Supporting Information, Table 3S), suggesting an energy-speed-precision trade-off as previously reported[19] (data presented are MEAN ± SEM, $n = 4$, $*p < 0.02$).

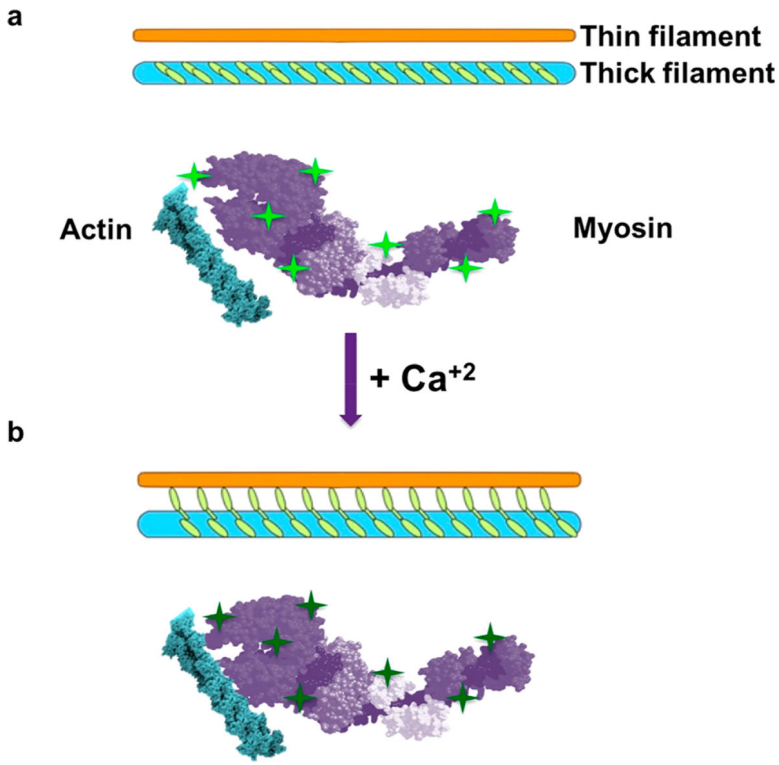

Figure 5.

Schematic diagram showing myosin heads in the thick filament unwind and loses enthalpy in the presence of calcium, resulting in increased interactions with the thin filament. (a) Thick and thin filaments before calcium addition. Note the bright green fluorescing QDs (bright green stars). (b) Calcium addition results in the loss of alpha helical content of myosin molecules demonstrated using CD and the consequent release of heat and therefore loss of QD fluorescence (dim green stars). Loss in alpha helical content of the myosin molecule in the presence of calcium could result in a radial increase in size of the molecule, enabling myosin heads greater probability to interaction with actin in the thin filament.